Developments in the Built Environment 15 (2023) 100170

Contents lists available at ScienceDirect

Developments in the Built Environment

journal homepage: www.sciencedirect.com/journal/developments-in-the-built-environment

Damage detection in a RC-masonry tower equipped with a non-conventional TMD using temperature-independent damage sensitive features

Eleonora M. Tronci [a,*], Raimondo Betti [a], Maurizio De Angelis [b]

[a] Department of Civil Engineering and Engineering Mechanics, Columbia University, New York, USA
[b] Department of Structural and Geotechnical Engineering, Sapienza University of Rome, Rome, Italy

A B S T R A C T

Many features used in Structural Health Monitoring strategies are not just highly sensitive to failure mechanisms, but also depend on environmental or operational fluctuations. To prevent incorrect failure uncovering due to these dependencies, damage detection approaches can use robust and temperature-independent features. These indicators can be naturally insensitive to environmental dependencies or artificially made independent. This work explores both options. Cointegration theory is used to remove environmental dependencies from dynamic features to create highly sensitive parameters to detect failure mechanisms: the cointegration residuals. This paper applies the cointegration technique for damage detection of a concrete-masonry tower in Italy. Two regression models are implemented to capture temperature effects: Prophet and Long Short-Term Memory networks. Results demonstrate the advantages and limitations of this methodology for real applications. The authors suggest to combine the cointegration residuals with a secondary temperature-insensitive damage-sensitive set of features, the Cepstral Coefficients, to address the possibility of capturing undetected structural damage.

1. Introduction

Vibration-based Structural Health Monitoring (SHM) seeks to efficiently identify damages and anomalies in a structure's performance by analyzing its recorded vibrations. Such approaches search for any changes in the regular pattern of a structure's behavior, assuming that any deviation from its current or future performance is due to variations in its material and/or geometric properties caused by damage (Farrar and Worden, 2012) that will hinder its current or future performance (Farrar and Worden, 2012). This alteration will be reflected in the structural behavior, but it can be clearly recognized through continuous monitoring the healthy state since this deviation exists only with respect to a reference condition.

These strategies have been widely studied and innovated in the literature with regard to multiple focusing areas: optimizing sensor placement (Civera et al., 2021), utilizing modern sensor systems (Barsocchi et al., 2021), combining different monitoring approaches (Ierimonti et al., 2022). These innovations are critical in designing reliable and accurate damage detection strategies, especially for historical structures that have withstood the test of time (Pallarés et al., 2021). Due to the prevalence of masonry structures in Italy, numerous publications have focused on developing and applying identification techniques to this typology of structures, offering a unique set of vibration-based monitoring applications that address the different challenges and the dynamic characterizing behavior of masonry systems (Gentile and Saisi, 2007; Cabboi et al., 2017; Ubertini et al., 2017; Kita et al., 2019; Invernizzi et al., 2019; Tronci et al., 2020a).

For the SHM research community, the investigation and search for features highly sensitive to damage has been a primary topic of interest and led to a rich literature production and to a broad experimentation of new damage indicators (Tronci et al., 2022; Li et al., 2023; Quqa et al., 2021; Bernagozzi et al., 2021). However, SHM strategies based on the observation of damage sensitive features over time often assume that changes in a structure's mechanical properties are solely caused by damage variations, which is not the case. Environmental and operational conditions inevitably affect structural behavior, as seen in several studies (Han et al., 2021). Intuitively, factors like temperature and humidity fluctuation may change the material properties and the geometry characteristics of a structure. It is essential to keep in mind that the variation caused by environmental and operational changes could be, in some cases, comparable or more prominent than those due to damage, and consequently, they could hide damage occurrence and give false information about the structural health.

Therefore, the environmental influence on the structure needs to be

* Corresponding author.
E-mail address: et2501@columbia.edu (E.M. Tronci).

https://doi.org/10.1016/j.dibe.2023.100170
Received 12 March 2023; Received in revised form 23 April 2023; Accepted 4 May 2023
Available online 18 May 2023

taken into account when applying any vibration-based damage detection methodology. This necessity can be addressed at different levels and in multiple ways. The most popular approaches rely on models that learn the patterns in the structural behavior of structures associated with the environmental and operation conditions (García-Macías and Ubertini, 2022; Silva et al., 2021; Ubertini et al., 2017; Cross et al., 2012) and eventually remove these dependencies from the desired choice of damage indicators creating a robust damage sensitive feature. An alternative option consists of looking for features that are naturally independent of those fluctuations and changes and tend to be sensitive mainly to damage.

This work explores both possibilities. First, the cointegration technique is implemented to remove the environmental dependency from modal tracking quantities such as frequencies. Cointegration is a widely used tool in econometrics to eliminate trends from data. The theoretical background of the approach draws from several key texts from the econometrics literature (Johansen, 1995; Fuller, 2009; Cross et al., 2011), which the reader may refer to for a more mathematically rigorous treatment of the material. The cointegration technique appears to be very useful in the data normalization phase of SHM, as it looks to remove the environmental and operational effects intertwined with longer time scales compared to the dynamics of the structure sensitive to damage. If two or more monitored variables from a monitored system are cointegrated, then it is possible to find some combination of them that will be stationary. Then, the stationary residual created from the cointegration procedure can be used as a damage sensitive feature (DSF) independent of the normal environmental and operational conditions.

Cross et al. (2011) proved the effectiveness of linear cointegration in SHM and later proposed an alternative nonlinear cointegration that considers the nonlinearity of the relationshipbetween variables (Shi et al., 2016). Coletta et al. (2019) successfully applied the cointegration technique to remove environmental trends in the case of a historical masonry Sanctuary using nonlinear regression models like Support Vector Machine and Relevance Vector Machine. Recently, Turrisi et al. (2022) provided an application of the linear correlation applied on a complex structure of a singular nature, the steel roof of the G. Meazza stadium in Milan.

This work considers two models designed to account for the seasonality and time-dependency of environmental temperature conditions, Prophet and Long Short-Term Memory (LSTM) regression model. The methodology is validated using the data collected on a reinforced concrete masonry Civic Tower in Italy.

The results show the conditions in which cointegration successfully removes environmental dependencies from structural frequencies, enhancing their damage detection capability. The work also presents a real damage case scenario where cointegration fails to achieve the goal. To overcome the limitations of this technique, the study proposes an alternative damage sensitive feature option: Cepstral Coefficients (CCs). These parameters are adapted from Mel Frequency Cepstral Coefficients (MFCCs), which are well-known in the speech and speaker recognition research field. However, their modification and use as DSFs for damage detection in civil structures are relatively new (Tronci et al., 2022; Li et al., 2023; Balsamo et al., 2013, 2014). The CCs have several interesting characteristics, and their extraction process, built on simple means of digital signal processing operations, differs significantly from the complex and sophisticated structural identification algorithms adopted to extract the modal parameters of structures. The results obtained on the monitoring data of the Civic Tower of Rieti address the reliability of CCs as DSFs, focusing on their ability to distinguish between damage changes and environmental fluctuations.

2. Cointegration strategy to derive temperature-independent damage sensitive features

Cointegration is a powerful tool that can be used to remove trends in SHM data to identify a stationary feature related to the structure's health. Starting from a set of nonstationary time series that represents the evolution of the dynamic response of the system over time (e.g., accelerations, frequencies, etc.), the cointegration aims to define a combination of them which is stationary. Then, the stationary residual can be used as a DSF independent of the normal environmental and operational conditions.

To measure the extent of the nonstationarity of a time series, it is useful to introduce the so-called order of integration. A nonstationary time series $z(t)$ is said to be integrated of order p, i.e., $I(p)$ if its p-th difference is stationary. For example, the given time series $z(t)$ $I(1)$ must be differenced only once to obtain a stationary process, which will then be $I(0)$. The cointegration technique can be easily implemented in damage detection approaches, and here it is considered in an outlier-based methodology consisting of four main steps.

Step 1: Initially, the order of integration of the monitored damage sensitive features needs to be checked to establish if they are suitable to be normalized using the cointegration approach. The Augmented Dickey-Fuller (ADF) test is initially run on each variable. Each variable should be integrated of the same order to be a candidate. The reader is referred to (Fuller, 2009) for a detailed treatment of the ADF test.

Step 2: Once the suitable variables are identified, it is necessary to split the dataset into training and test sets. The regression model is then built using the training data. The training dataset should collect most of the possible fluctuations due to environmental variations to create a reliable and accurate regression model able to mimic the behavior of the structure during all the common operational conditions.

Step 3: Considering the training data, the relationships between the variables matching the ADF requirements are investigated. The construction of the regression model depends on how the different variables are correlated, particularly if these relationships are linear or nonlinear. Depending on how they are correlated, it is possible to choose the most suitable regression model for the study case. One variable is selected as the regression target, and the others are used to fit the model.

The model's performance is tested on the training data, and the residual series obtained from the predicted and measured data is evaluated using the ADF test. The cointegrating relationship is successfully established, and the common trends are purged if the model residual series is integrated to a lower order than the original variables. Therefore, the model residual series may be a potentially good temperature-independent indicator of damage-induced variations.

Step 4: Once a suitable regression model has been found, new data from the monitored variables should be projected onto it. If the cointegrating vector was established on data from the normal condition of the structure, the residual sequence would continue to be stationary all the time the structure operates in its normal state. When the monitor residuals deviate from the stationary known sequence, that change could be caused by the occurrence of structural damage.

2.1. Regression models

In this work, two different models are considered and tested as regression models to be used within the cointegration approach. In the past years different options have been considered to address linear and nonlinear types of correlations. Coletta et al. (2019) adopted the Support Vector Regression (SVR) and Relevance Vector Machine (RVM) algorithms in order to address the nonlinear correlation that sometimes can affect the structural frequency dependency on temperature. The nonlinear dependency in this case is accounted for through the use of a

kernel. However, both these regression methods are not structured to be time-dependent and are not specifically designed to address seasonality or long and short-term dependencies. To account for these two aspects, in the present work two different models are considered for the regression models. First, a forecasting model known as Prophet is considered. Then, a specific type of Neural Network is picked to build the regression model used in the learning task of the presented methodology, the Long Short-Term Memory networks.

Prophet was developed by Facebook's Data Science Team in 2017 (Vishwas et al., 2020; Taylor and Letham, 2018). It uses a data-adaptive decomposable additive time series model (Harvey and Peters, 1990) with three main model components: trend, seasonality, and holidays. The model can be expressed as the combination of the following terms:

$$y(t) = g(t) + s(t) + h(t) + \varepsilon_t \tag{1}$$

where $g(t)$ is the trend function which models the long-term non-periodic changes in the data, such as growth or decline; $s(t)$ is the seasonality that represents periodic changes (weekly, monthly and yearly cycles); $h(t)$ are the effects of the holiday which occur on potentially irregular schedules; and ε_t is an error term that is not accommodated by the model respectively. Prophet can model both linear and nonlinear trends, and can automatically detect changepoints where the trend changes. Using time as a regressor, Prophet is trying to fit several linear and nonlinear functions of time as components. Two trend models that cover Facebook applications are: a nonlinear saturating growth model and a piecewise linear model. Finally, Prophet can model both additive and multiplicative seasonality, and can handle complex seasonality patterns with Fourier series. The model is fitted by minimizing a loss function that measures the difference between the observed data and the predicted values. The reader is referred to (Vishwas et al., 2020) for a more detailed treatment of the subject.

Strategies based on the use of Neural Networks (NNs) have become extremely popular in the past years, particularly for time series modeling for SHM purposes (Li et al., 2023; Tronci et al., 2022; Giglioni et al., 2023; Pan et al., 2023; Eltouny and Liang, 2023). Within the family of NNs, Long Short-Term Memory is a type of Recurrent Neural Network that is designed to better handle long-term dependencies and memory-related problems. They were introduced by Hochreiter & Schmidhuber (Hochreiter and Schmidhuber, 1997), and were refined and popularized by many people in the research literature. The main idea behind LSTM is to control the flow of information through the network using a series of gates that selectively allow or prevent information from passing through. This capability allows LSTM to be effective in modeling time series data, natural language processing, and other applications that require processing sequential data.

The performance of these two models in the creation of a robust and reliable regression model will be compared with SVR and RVM in terms of Root Mean Square Error (RMSE) and Relative Root Mean Square Error (RRMSE), and the best performative model will be later on used to implement a damage detection strategy.

3. Cepstral Coefficients as natural damage sensitive features

Mel-Frequency Cepstral Coefficients are features widely used in the field of speaker and speech recognition, and they differ from the other common DSFs, such as modal frequencies, as they allow for consideration of the response property in both the frequency and time domain simultaneously. These MFCCs are defined as the inverse discrete cosine transform of the log-modified spectrum of the system response.

The cepstrum was originally developed to filter the effects of echoes from time series, and it was first introduced by Bogert (1963) and his colleagues at Bell Laboratories in 1963. The discrete-time formulation of the cepstrum and its complex counterpart, the complex cepstrum, were later addressed by Oppenheim (Oppenheim et al., 2001). In 1980, Davis and Mermelstein (1980) proposed a compact version of the cepstrum that used the Mel-spectrum to obtain the cepstral representation of speech signals. The set of coefficients extracted from the sampled speech signal was called Mel-Frequency Cepstral Coefficients.

These coefficients present explicit relations to poles and zeros of the system transfer function leading to the speculation that a strong relationship must exist between such coefficients and structural properties. These features require very low user expertise to be extracted and analyzed, making them particularly convenient for implementing automatic SHM procedures.

The first application of these coefficients for civil engineering studies was given by Zhang et al. (2011), who used MFCCs to detect concrete delamination on a bridge deck by analyzing the MFCCs extracted from records of the impact sound produced by impacting the surface of the concrete slab with a steel bar.

In this work, the Cepstral Coefficients are investigated. They are the results of the adaptation of MFCCs proposed by Balsamo et al., 2013, 2014, implemented to make these features suitable for civil structures. These features are extracted directly from the time histories of the structural response and were successfully used in a statistical pattern recognition approach to infer damage occurrence.

The Cepstral Coefficients can be extracted from a sampled signal or time history, $x[n]$, performing a sequence of six steps involving simple signal processing tools which make the extraction process extremely easy, quick and, user-friendly (Fig. 1); the reader is referred to (Beigi, 2011) and (Balsamo et al., 2014) for a detailed treatment of the subject.

In the preliminary step, each time history is divided into a number of frames, N_{frames}, where each frame must be long enough to be considered stationary and consists of a certain number of samples ($N_{samples}$). In order to reduce the riddle effects on the frame spectra due to the segmentation procedure, a non-rectangular window (usually Hamming window) is applied to each frame.

Afterward, applying the Discrete Fourier Transform (DFT), the Power Spectrum (PS) is evaluated for each frame, obtaining, for each time history, N_{frames} PS segments. To emphasize the parts of the spectrum that are more likely to be expressing the structural behavior, a *frequency warping* procedure is performed. It allows the user to modify and scale the linear frequency scale to weigh more the area of the spectrum with the greatest energy content. The new modified frequency scale and the linear frequency scale are almost equivalent up to a cutoff frequency of f_c, after which their relation becomes logarithmic. The user is in charge of defining the cutoff parameter, which can be set by observing the frequency content of the system. It should be chosen as the upper limit of the meaningful frequency range where most of the structural frequency contribution lies. Averaging the spectra of all the PS segments results in the generation of what will be referred to as an *average spectrum* (Fig. 2). The average spectrum highlights the frequency range within which the most significant frequency content is observable. The cutoff frequency is then chosen as the upper bound of that portion of the averaged spectrum. This new scale mimics the trend of the Mel-scale (Beigi, 2011), working on a frequency range compatible with structural problems, according to the following expression:

$$\widetilde{f} = f_c \log_2\left(1 + \frac{f}{f_c}\right) \tag{2}$$

The frequency warping step is performed by grouping together the power spectrum values into M frequency bands and weighting each group by a triangular weighting function (Fig. 2). According to the Fraile

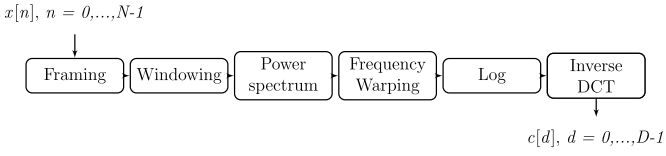

Fig. 1. Cepstral Coefficients s extraction process.

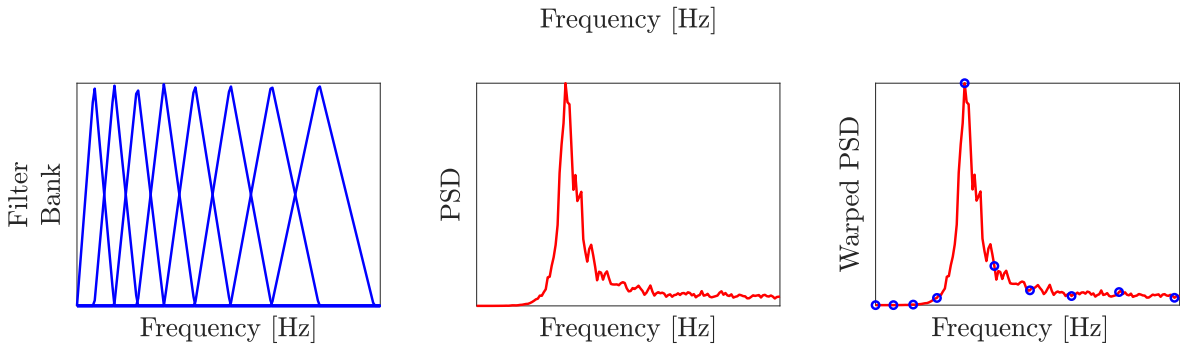

Fig. 2. Frequency warping procedure for the *i*th frame.

et al. criterion (Fraile et al., 2008), M can be set equal to $3ln(f_s)$, where ln () represents the natural logarithm operation, while f_s is the sampling frequency. This is a common relationship in the speaker recognition research field, and that can also be adopted for structural problems. The triangular filters are constructed such that their centers are equally spaced on the frequency scale $(\widetilde{f})$ given in Eq. (2), with each filter being symmetric with respect to its center (Fig. 2).

The power spectrum of each frame is weighted, multiplying it by the triangular filter corresponding to each mth frequency band (Fig. 2), with $m = 1, 2, .., M$. After that, each contribution coming from this multiplication is summed along the frequency range leading to the matrix N_{frames} vectors, for the single frame, of dimensions $M \times 1$, which contains the warped power spectrum or modified spectrum. This is a synthetic representation of the frequency content of the system, where the mth element carries on the portion of the spectrum collected by the mth filter and tells how this element contributes to the overall frequency content.

The Cepstral Coefficients extraction procedure is completed by applying a D-points Inverse Discrete Cosine Transform (IDCT) (Fig. 3a) to the logarithm of the modified spectra (Fig. 3a):

$$c[d,k] = \sum_{m=0}^{M-1} a_m \ln(H[m,k]) cos\left[\frac{\pi(2d+1)m}{2M}\right] \quad \text{for } d = 0,\ldots,D-1 \text{ and for } k = 1,\ldots,N_{frames} \tag{3}$$

where a_m is equal to $\frac{1}{M}$, for $m = 0$, and to $\frac{2}{M}$ otherwise. $H[m]$ represents the mth point of the modified spectrum, where $m = 0, \ldots, M-1$ while $c[d]$ is the dth Cepstral Coefficient, which could be collected in a coefficient vector for each kth frame $\mathbf{c}(k) \in \mathbb{R}^{D\times 1}$. The number of CCs is chosen arbitrarily, but commonly is selected equal to the number of M frequency bands already defined.

Computing the coefficients of IDCT independently for each Cepstral Coefficient (Fig. 3a), it is possible to appreciate better how these coefficients modify the different frequency contributions of the new modified log spectrum.

$$c_{IDCT}[d] = \sum_{m=0}^{M-1} a_m cos\left[\frac{\pi(2d+1)m}{2M}\right] \quad \text{for } d = 0,\ldots,D-1 \tag{4}$$

Cepstral Coefficients are always real and convey information about the physical aspects of the signal. When $d = 0$, the cosine term of the Discrete Cosine Transform (DCT) becomes 1 and, consequently, the first Cepstral Coefficient c_0 is the average power of the signal. A negative coefficient relates to the local minimum of the cosine in the DCT noting that the higher frequency indices in the summation of the DCT are contributing more. On the other hand, a positive peak means that there must be more power in the lower frequency range. As the dimension d of CCs becomes larger, the number of alternating partitions in the

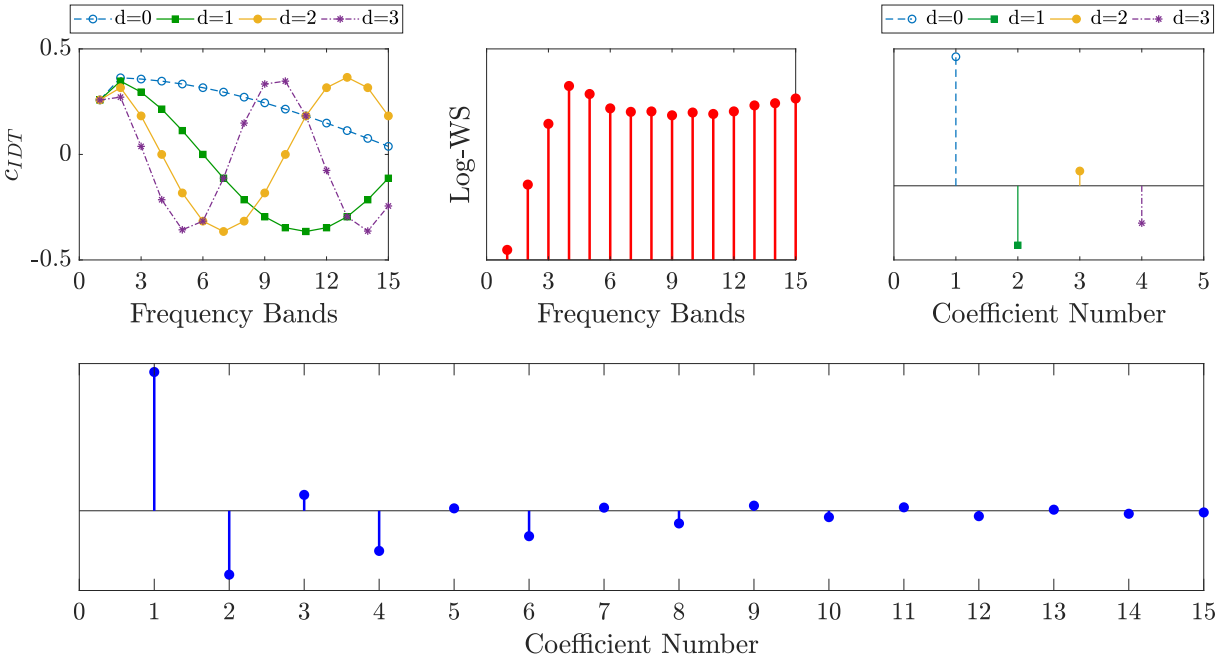

Fig. 3. Extraction of the Cepstral Coefficient vector: (a) Application of the first six coefficients of the IDCT to the Log-Warped spectrum; (b) Cepstral Coefficients vector for the *i*th frame.

frequency range increases.

It is precisely this last characteristic that gives CCs the the potential to discriminate between the trends in data due to environmental and operational variation and the alterations caused by damage. The application of the higher-order DCT coefficients allows for natural detrending of the coefficients, because the contributions from the frequency bands carrying the environmental information cancel out with each other in the summation.

The IDCT can be thought of as a filtering process that removes high-frequency components from the signal, thereby smoothing it and reducing its complexity. This is because the DCT tends to concentrate signal energy in lower-frequency components, while high-frequency components are attenuated. By applying the the IDCT, high-frequency components are amplified and added back to the signal, effectively smoothing and filtering it.

4. Description of the Civic Tower and its monitoring system

The Civic Tower, erected in 1940 (Fig. 4a), is located in the civic center of Rieti. It is a part of the larger Town Hall of Rieti building, built in the XIII century. The Civic Tower is rigidly connected on the east and north sides to the Town Hall, with the connection obtained through the floor diaphragm continuity at the second, fourth, and fifth floors and through the shared internal load-bearing walls. The Tower has an approximately square plan of dimensions 14.00 m × 13.70 m and an overall height of 32 m. It consists of seven floors above ground, including the roof level, a level on the ground floor covered by a portico with vaulted ceilings, and a basement level.

The porch located on the ground floor is made of blocks of solid travertine and concrete mortar within the blocks. The lofts at the underground level consist of alternate layers of concrete tiles and slabs, while the ones at the upper levels consist of cement rafters and hollow block slabs. The external structure consists of masonry walls with coating blocks of travertine, which have a thickness comparable to that of the masonry section. The thickness decreases from 1.00 m (first floor) to 0.60 m (top floor). Inside, there is a reinforced concrete frame with four columns. The dimensions of the columns vary along with the height (1.00 m × 1.00 m on the first floor and 0.40 m × 0.40 m on the penultimate one), while the section of the beams is fixed at 0.50 m × 0.50 m.

In 2014, a non-conventional Tuned Mass Damper (TMD) system was installed on the Civic Tower to reduce its seismic vulnerability. The TMD system provides supplemental damping by inducing vibration energy transfer from the structural portion below the isolation system to the structural portion above the isolation system.

A long-term monitoring system was installed on the Civic Tower to monitor its dynamic behavior and health condition during normal operations. The data acquisition system is an HBM MCGPlus, with the control unit AB22A, linked to a PC running the acquisition software HBM Catman 5.0.

The monitoring of the Civic Tower has been conducted in three separate phases where structural accelerations were measured in 5 min-long recordings with a sampling frequency of 100 Hz, using a sensor network that consists of piezoelectric model PCB 393A03 uni-axial accelerometers (1 V/g sensitivity). The first phase consists of five daily monitoring campaigns carried on between July 2015 and January 2016, which is fundamental in defining a baseline sensor setup for all future campaigns. The reference sensor setup, which better catches the tower's dynamic behavior, consists of six high-sensitivity piezoelectric uni-axial accelerometers: three accelerometers (Fig. 4c) placed on the floor supporting the TMD system and the remaining three on the TMD mass.

The second monitoring phase started on August 24th, 2016, right after the earthquake that struck the small town of Amatrice and the surrounding areas. At this time, the acquisition system was set alternatively in continuous mode, 24 h a day, measuring 5 min long records. The program also had a standby trigger mechanism to detect any sudden accelerations. Finally, during the last phase from December 2017 until January 2019, the monitoring system collected eight ambient vibration recordings (5 min long) per day at four different times of the day: 7:00 a.m., 1:00 p.m., 7:00 p.m., and 1:00 a.m. In this work, the monitoring data from only the last phase will be used. More information on the structure, the experimental setup and the monitoring campaigns can be found in (Tronci et al., 2020a).

The structure's dynamic behavior is represented by its modal parameters: frequencies, damping ratios, and mode shapes. These features are extracted from the 5 min long AVTs data recorded during the monitoring campaigns using a semi-automated identification procedure based on Data-Driven Stochastic Subspace Identification (DD-SSI) technique developed by the authors (Tronci et al., 2020b). The reader is referred to (Tronci et al., 2020a) for a detailed description of the adopted framework and the parameters used in this case study.

5. Cointegration residuals as damage sensitive features

Fig. 5 shows the time histories of the identified natural frequencies obtained by applying the semi-automated DD-SSI output-only modal

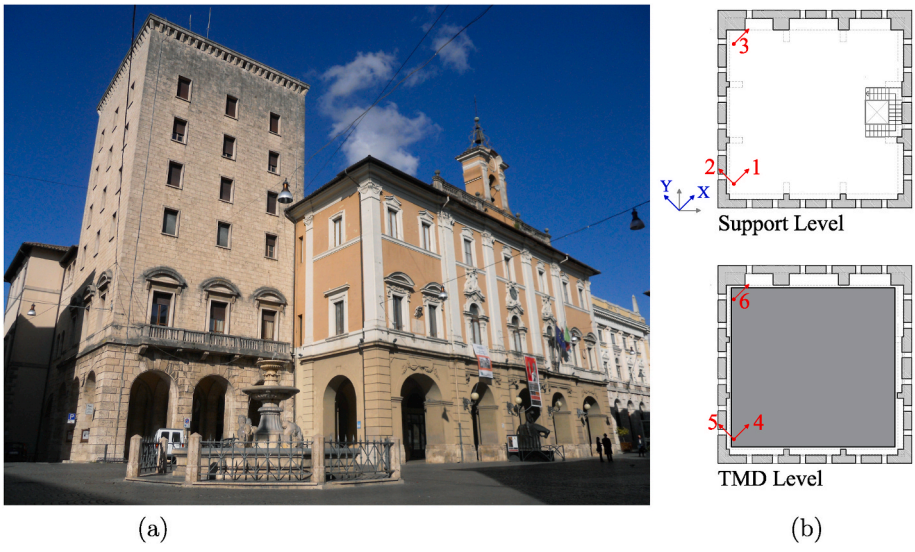

Fig. 4. View the Civic Tower: (a) the Town Hall complex, (b) the Civic Tower, (c) the sensor setup.

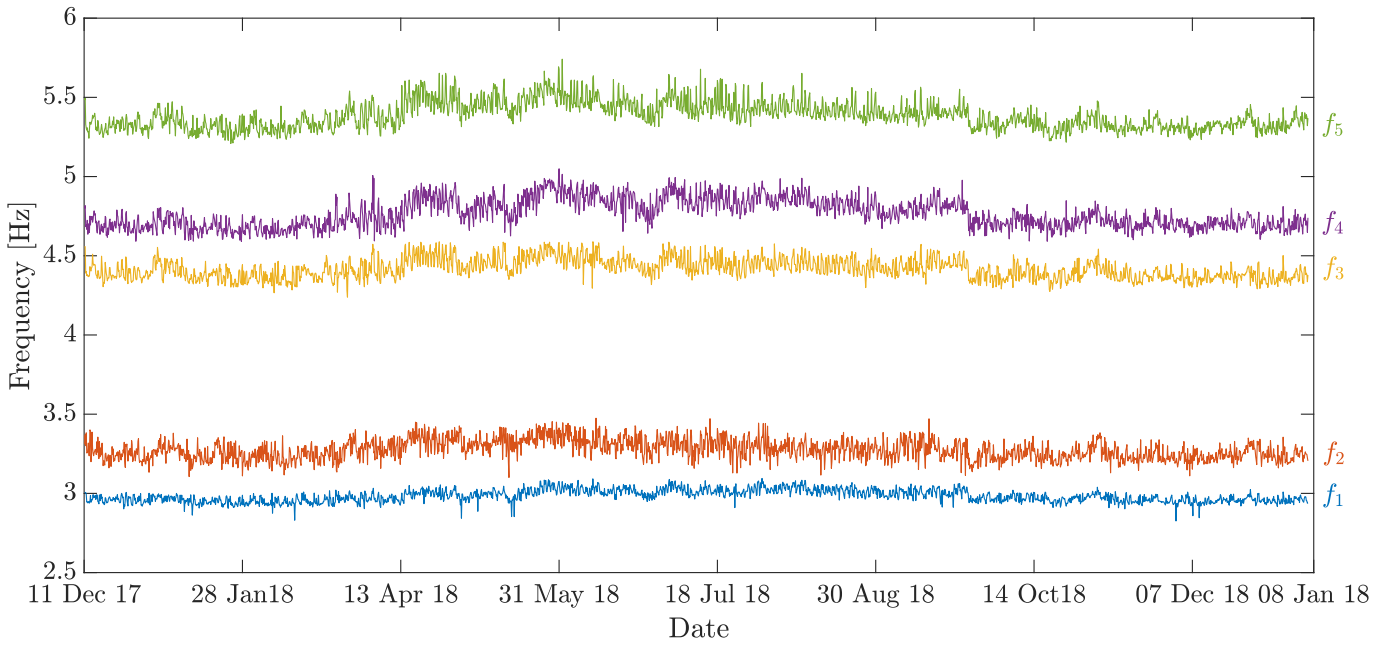

Fig. 5. The five structural modes identified in the third monitoring phase for the Civic Tower of Rieti.

identification technique mentioned in the previous section.

The time evolution of the modal frequencies during the third monitoring phase, from December 2017 to January 2019, is shown considering the four records collected per day. Five modes are successfully identified in most of the dataset: the first two translational modes, f_1, and f_2; the third and fourth coupled modes, f_3 and f_4; and finally, the fifth torsional mode, f_5. Significant seasonal increases in the structural frequencies from winter to summer are visible in Fig. 5; such increments are conceivably associated with changes in environmental conditions, with ambient temperature being the most prominent factor. It is noted that the increase of natural frequencies with temperature is caused by a stiffening effect associated with the closing of microcracks within mortar layers due to thermal expansion. Conversely, the reduction of frequencies related to a lower temperature is caused by microcracks opening (Tronci et al., 2020a).

Following the steps presented in the methodology section, the order of integration of the frequency trends was investigated to ensure that cointegration could be adopted in this case. The ADF test established that all the frequencies were nonstationary. Furthermore, after applying the difference operator only once, the same test determined their stationarity to a 95% confidence level. Consequently, it is reasonable to expect an integration order equal to 1 for all the five frequencies inspected.

Subsequently, the portion of data used to carry on the training is identified. This case study shows how the structural modes present a higher seasonal fluctuation between the beginning of April 2018 and mid-July 2018. Therefore, to build a robust regression model able to catch the behavior of the tower under environmental changes properly, 1000 observations have been picked for training the model between April 20th, 2018, and July 18th, 2018.

Once the training set has been chosen, it is necessary to explore how the different variables are correlated, particularly if these relationships are linear or nonlinear. This can be achieved by adopting various measures of correlation. In this work, different correlation coefficients are considered (Fig. 6): the Pearson correlation coefficient C_P is a measure of the strength of a linear association between two variables; the Spearman's correlation coefficient, C_S assesses monotonic relationships (whether linear or not); the distance correlation, C_D, is a measure of association strength between both linear and nonlinear random variables; the maximal correlation, C_{MC}, that does not require assumptions

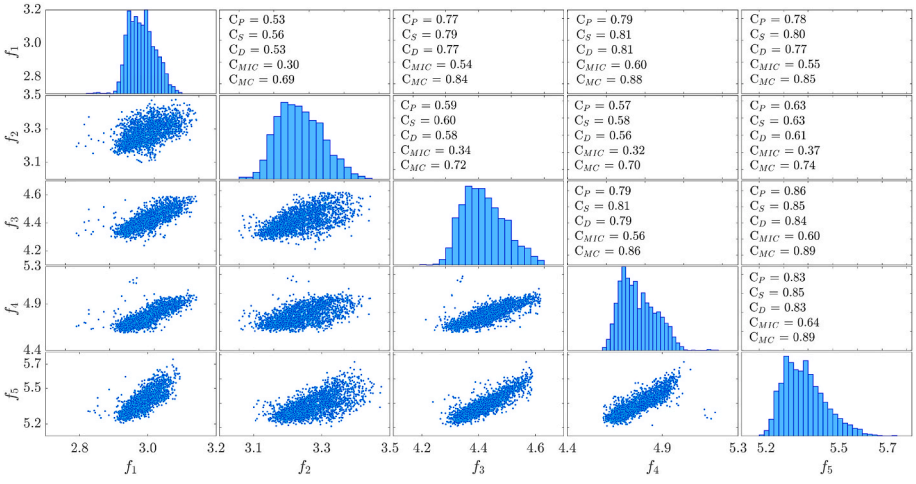

Fig. 6. Matrix of the correlation coefficients for the five structural frequencies.

on the data distribution and can detect nonlinear correlations, and it is very efficient and robust to noise; the maximal information coefficient, C_{MIC}, is a measure of the strength of the linear or nonlinear association between two variables.

For the Civic Tower of Rieti, a linear relationship between the variables emerges consistently by looking at the correlation coefficients for all the frequencies except for the second structural mode, which presents a low correlation independently from the linear or nonlinear nature of the other modes. Consequently, only the first, third, fourth, and fifth structural modes are considered when building the regression model.

For the sake of brevity, the results reported in this work correspond to the regression on the fifth frequency, f_5, which is selected as the target mode, while the remaining three frequencies are used to fit the model. The regression model is built using a network consisting of four layers: a sequence input layer, an LSTM layer, a fully connected layer, and a regression output layer. The size of the sequence input layer corresponds to the number of features of the input data used in the regression, which is three in this study case. The LSTM layer has three hidden units, followed by a fully connected layer equal to the number of responses or target features, one, in this case. The training is carried on for 100 epochs with mini-batches of size 32 using the Adam optimizer, with a learning rate of 0.01.

In the case of Prophet, four main parameters could be tuned. The changepoint prior scale which controls how flexible the trend is and how much it can change at the changepoints (the points in a time series where there is a change in the statistical properties of the data, such as the mean, variance, or trend). A higher value allows more changepoints and a more flexible trend. The second parameter is the seasonality prior scale which controls the strength of the seasonality model. A higher value allows the model to fit larger seasonal fluctuations; a lower value dampens the seasonality. It is also possible to set the holidays prior scale that controls the strength of the holiday components model. A higher value allows the model to fit larger holiday effects; a lower value dampens them. Finally, it is possible to set the seasonality mode, which determines whether the seasonality components are modeled additively or multiplicatively to the trend.

For the study case application presented in this work, cross-validation for the different training set options was considered varying the two main parameters of interest: the scale on the changepoint and the scale on the seasonality. They were considered to vary in the following ranges [0.001, 0.01, 0.1, 0.5] and [0.01, 0.1, 1.0, 10.0], respectively. The scale on holiday is ignored, and the seasonality mode is kept additive, given that the observed seasonality trends were mainly linear from previous studies conducted by the authors (Tronci et al., 2020a). The results from the cross-validation indicated the independence of the results from these parameters, showing the default flexibility of the model to maximize the learning of dependencies from the training dataset. Therefore, no particular parameter was specialized, and the default settings were considered.

An initial sensitivity investigation focused on the influence of the time window and number of data points used to train the algorithms. Four different time windows were considered, starting at four different phases of the year: the first (T1) started on January 12th, 2018, the second (T2) on April 1st, 2018, the third (T3) on May 1st, 2018, and the last one (T4) on July 18th, 2018. Given these options, five sets of cases were considered, with the number of observations for training equal to 300, 500, 700, 900, and 1100, respectively. Fig. 7 shows the results in terms of Relative Root Mean Squared Error for the training and testing datasets for all learning options.

The first evident result is the overall performance of the two models. While LSTM exhibits consistent and stable behavior between the training and testing datasets, leading to comparable low percentages of errors (between 0.8% and 1.3%), Prophet exhibits less robust behavior, with highly performative results for the training set (error stays below 0.65%) but substantially worse results for the testing set (error reaches up to 9%). This suggests an overfitting tendency of the Prophet model, independent of the time window or number of observations used. No time window or number of observations led to substantially higher performance. The results presented in the following sections relate to the 1000 observations selected for training the model between the beginning of April 2018 and July 2018.

It is necessary to project new data onto the regression model and keep tracking the residuals over time to see if there is any deviation from the stationarity established in the training dataset. Introducing a control chart with an upper and lower threshold to bind the limits that identify the monitored system's normal condition can easily help spot any consistent deviation or anomaly. In this case, the upper and lower limits are considered as $\pm$ a certain number p of standard deviation σ with respect to the mean value of the residuals in the training dataset. The number p needs to be chosen so that almost all the residual values will fall between the control limits when the system is healthy. Here, the upper and lower limits are given for three values of p ($p = 1$, $p = 2$ and $p = 3$).

Figs. 8 and 9 show the results obtained using the Prophet and LSTM network to build the regression models for f_5. In Figs. 8 and 9, the first plot shows the identified frequency compared with the predicted one. In contrast, the second plot displays the model residuals with a constructed control chart that consists of the mean value of the residuals computed on the training dataset, the moving average of the residuals on a window of 30 points, and the lower and upper control limits for different

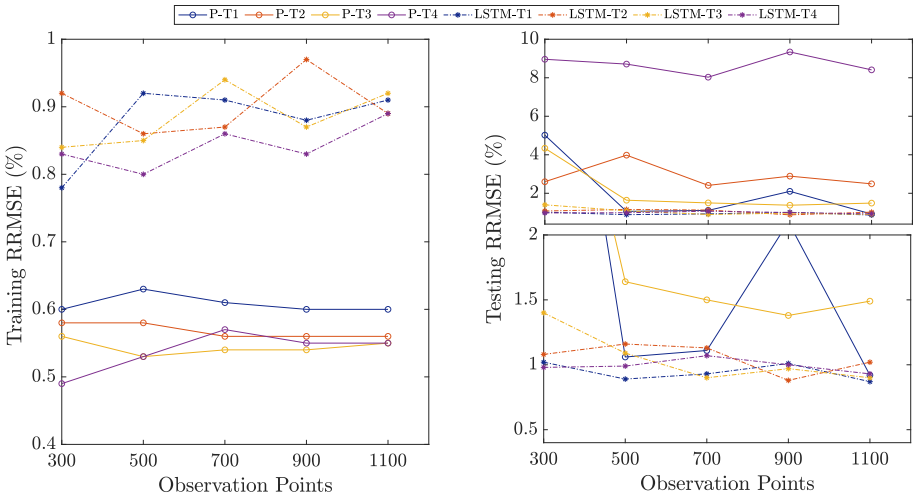

Fig. 7. Relative root mean squared error for LSTM and Prophet considering different time windows and number of data points.

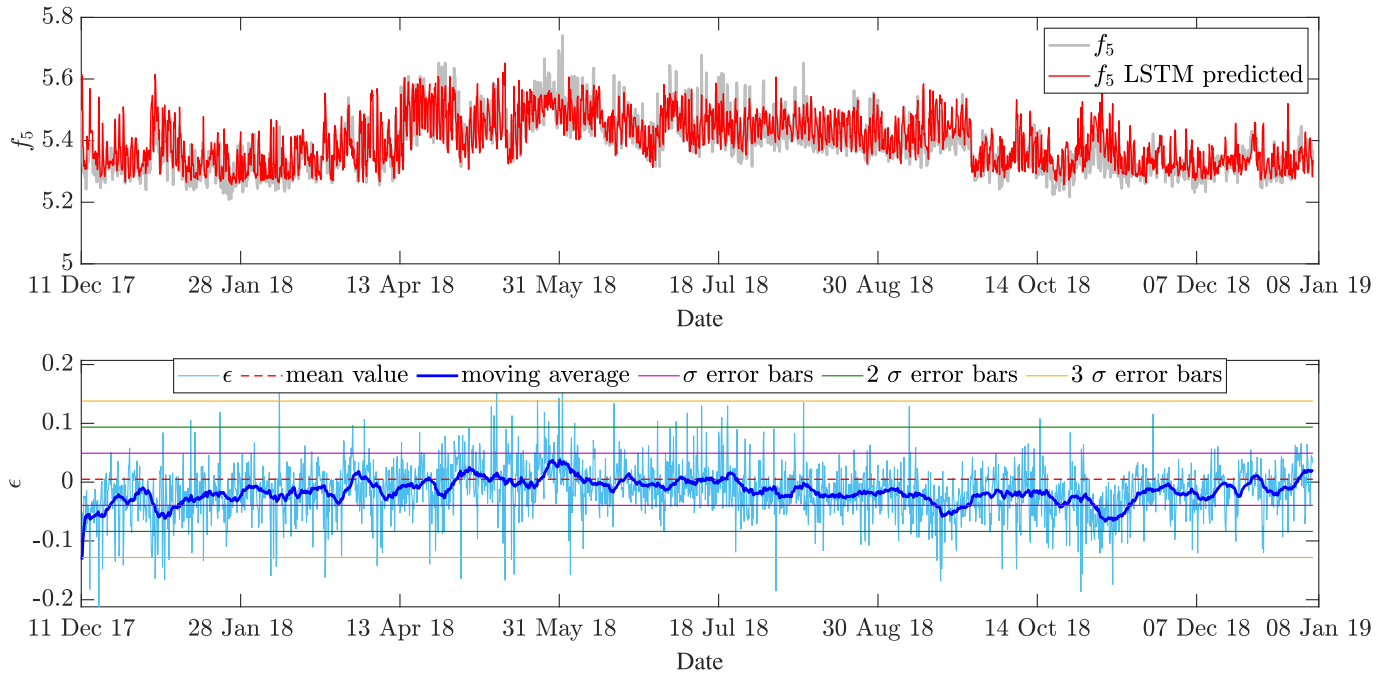

Fig. 8. LSTM model of f_5 using the collected data for f_1, f_3 and f_4.

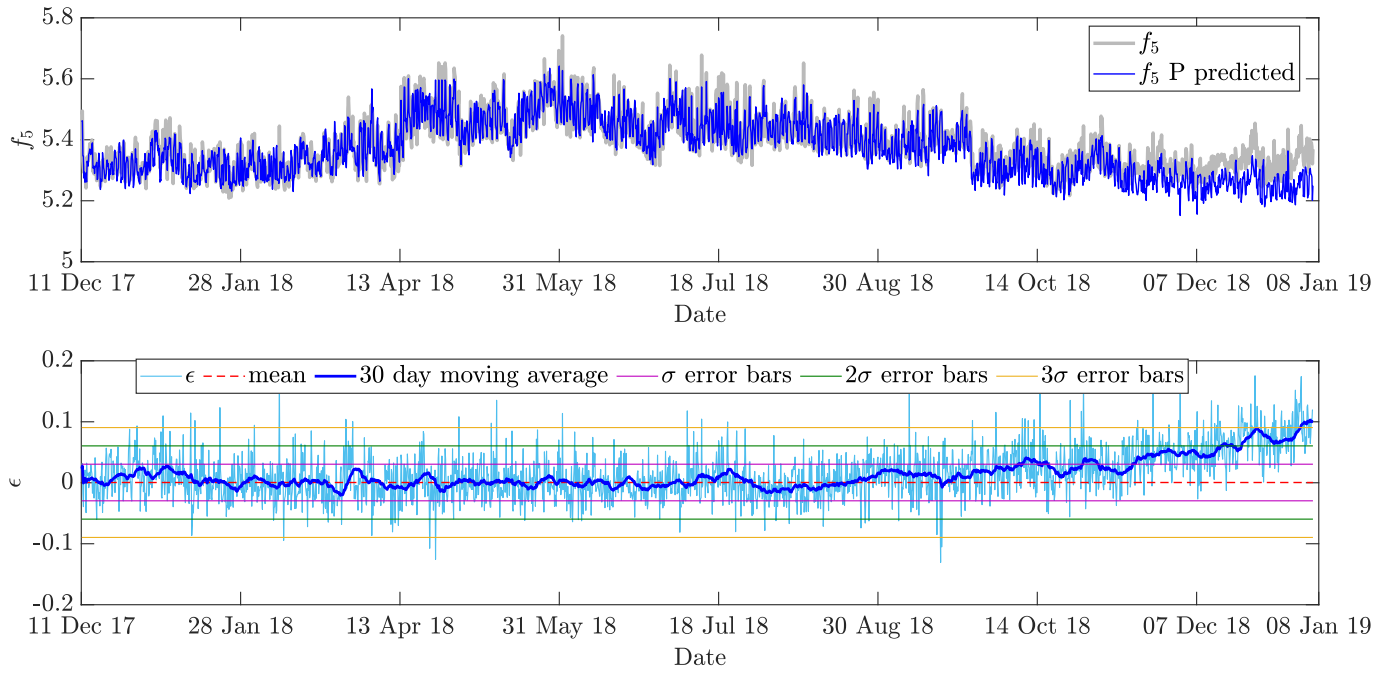

Fig. 9. Prophet model of f_5 using the collected data for f_1, f_3 and f_4.

confidence levels.

The ADF test performed on the residuals of the training dataset confirms the residuals' stationary and that the model residual series is integrated to a lower order than the original variables. Therefore, the cointegrating relationship is established successfully with common trends removed, making the model residual series a potentially good indicator of damage-induced variations.

Figs. 8 and 9 highlight the effectiveness of the regression model in removing environmental trends from the structural frequencies. In the case of the regression obtained using LSTM, a regular stationary trend can be observed in the residuals, with just a few points exceeding the upper and lower thresholds, which can be classified as false positive scenarios. The consistent stationarity of the residuals indicates an undamaged, healthy structural condition. Similar behavior is also exhibited by the residuals obtained using the Prophet model. However, towards the end of the monitoring period, the model's predictions diverge from the observations of the fifth mode. It is possible to observe that the frequencies converge to slightly lower values compared to those seen in the previous winter, diverging from the learned and observed annual trend on which the model was trained. The less satisfactory performance of the Prophet model in the final stages of the time history is caused by the lack of information in the training dataset. In this case,

the observations available for the model to learn are insufficient to capture the yearly linear trend caused by temperature properly. Therefore, the model is unable to catch the overall increase in the mean temperature over the year. The model would perform better with a longer training dataset covering approximately an entire year. This will be an investigation for future analysis when analyzing the observations beyond 2019.

Table 1 highlights the accuracy of the different regression models for the training and testing dataset. The results demonstrate the overall high performance of all the models creating a robust regression model for the fifth frequency as a function of the remaining ones. The testing results are all sufficiently consistent except for the outcomes provided by the Prophet algorithm. In this case, the RRMSE is distinctly higher with respect to SVR, RVM, and LSTM, and this is caused by the inability of the model to capture the final decreasing trend of the frequency in the winter time. SVM, RVM, and LSTM present a substantially more robust outcome. The LSTM model offers the possibility of having a long and short-term dependency that accounts for daily and seasonal fluctuations more structurally with respect to SVR and RVM that instead present no time-dependence memory.

The Civic Tower showed variations in its dynamic behavior, with significant reductions in its frequency values before and after the seismic events that happened in 2016 in the central region of Italy. On August 24th, 2016, the earthquake in Accumoli led to variations of the frequency average values before and after the shock ranging between 1% and 3% for the five structural frequencies. The reader is referred to (Tronci et al., 2020a) for more details on the behavior of the Civic Tower during the seismic events of 2016. A damage scenario has been simulated to test the robustness of the regression model within the cointegration technique to correctly spot anomalies in the system behavior. This is achieved by mimicking the reduction in the structural frequencies of the tower observed when a significant earthquake hit the structure in 2016. The anomalous condition (damage) is simulated by introducing a relative frequency change, Δf, in the five interested structural modes equal to the variations observed in correspondence of the earthquake that occurred in Italy's central regions on August 24th, 2016. The percentage variations correspond to 1.31%, 2.87%, 2.39%, 1.41%, and 1.95%, respectively for the five modes (Tronci et al., 2020a). The shift has been applied to the trend of the real frequencies starting from observation 1818 (October 17th, 2018) until the end of the dataset.

It can be noticed in Fig. 10 how the residual values, after the introduction of damage, deviate from the mean value, exceeding the threshold of σ error bars and 2σ error bars, with several points set below the threshold corresponding to 3σ error bars. Thus, the deviation from the regular behavior is permanent as opposed to the false positive cases, where the residuals converge back to the average values after briefly exceeding the more restrictive threshold. In this numerically damaged case, the cointegration achieves optimal performance in the removal of the temperature dependency for the fifth structural frequency, letting the damage occurrence easy to observe in the residuals.

An additional application of the cointegration strategy for damage detection is also considered using the real frequency series derived from the monitoring data collected on the tower that presents the true damage data. However, in order to maintain the damage occurrence towards the end of the monitoring period, the time axis of the data is inverted. In the real study case, the frequency variation due to damage is consistent in magnitude among all the frequencies, and there is no pronounced damage in any of the tracked modes. Given the persistent presence of damage in all the cointegrated variables, the variation due to damage is also captured by the regressor model, and the residuals consequently remove it, as can be observed in Fig. 11. The residuals, even if showing a pronounced divergence from the mean value, stay within the control limit thresholds associated with 3σ error bars. In this real study case, the cointegration technique shows its limitation in the creation of robust damage sensitive features.

Table 1
Root mean squared error and relative root mean squared error for different regression models for the training and testing dataset.

Model	Training		Testing	
	RMSE	RRMSE	RMSE	RRMSE
Support Vector Regression	0.036	0.66%	0.037	0.70%
Relevance Vector Machine	0.038	0.70%	0.040	0.75%
Prophet	0.033	0.60%	0.049	0.92%
Long Short-Term Memory	0.039	0.71%	0.040	0.74%

6. Cepstral Coefficients as alternative damage sensitive features

Coefficients have been extracted from the monitoring data recorded during three years. Before applying the extraction procedure discussed in Section 3, the number of triangular filters must be selected with the value for the cutoff frequency. The number of filters can be set according to the Fraile et al. criterion (Fraile et al., 2008); since the sampling frequency adopted to simulate the system response is equal to 100 Hz, M is set to 13. According to the observed frequency content of the tower, the cutoff frequency is set to 10 Hz. Consequently, the number of selected coefficients is chosen equal to the number of frequency bands.

Fig. 12 shows the frequency warping strategy implemented for the Civic Tower of Rieti. The power spectrum for the monitored structure is shown in the top plot, and it is possible to observe the five peaks corresponding to the main structural modes. The centroid of the triangular filters represented in the subplot below is also reported to overlap with the spectrum. The Figure highlights how the 4th, 5th, 6th, and 7th filters are the ones capturing and representing the majority of the energy content of the spectrum. The effect of the temperature and the long-term environmental component will reflect in these contributions over the monitoring period. This dependency is filtered out by applying the inverse discrete cosine transform in the case of the higher-order coefficients.

Fig. 13 shows the average time series of two coefficients extracted from channel 2. The coefficient c3 presents a main drop right after the earthquake series of shocks on January 18th, 2017. The epicenter of the seismic events was in Capitignano, which is 38.5 Km far from Rieti. Additionally, the third coefficient exhibits a seasonal trend that matches the temperature fluctuation observed in the frequencies. On the other hand, the eleventh coefficient c11, is consistently more stationary, revealing an important reduction after the earthquake occurred on August 24th, 2016, and a smaller jump in correspondence to the one that took place on January 18th, 2017. Unlike the third coefficient, c11, does not exhibit any seasonal changes remaining substantially stationary.

Fig. 14 shows the coefficient c11 included in a control chart similar to the one defined for the cointegration residuals. It is evident how the coefficient values stay stationary and confined within the control chart limit except for only one data point exceeding the 3σ error bars. Then, in correspondence with two of the three main seismic events that happened in the central area of Italy in 2016, the coefficients substantially deviate from the mean value associated with the undamaged condition.

7. Conclusion

The current study shows the accuracy of a damage detection approach in a real monitoring application by utilizing damage-sensitive features independent of long-term environmental trends. This work shows and compares the adoption of the cointegration residuals and the Cepstral Coefficients as damage sensitive features. The objective is to unfold the limitations that can arise in using temperature-independent residuals in real study cases and propose the Cepstral Coefficients as an alternative indicator to be used in addition and combination with the cointegration residuals.

In particular, the study examines the temperature and damage sensitivity of these two sets of features in a damage detection monitoring

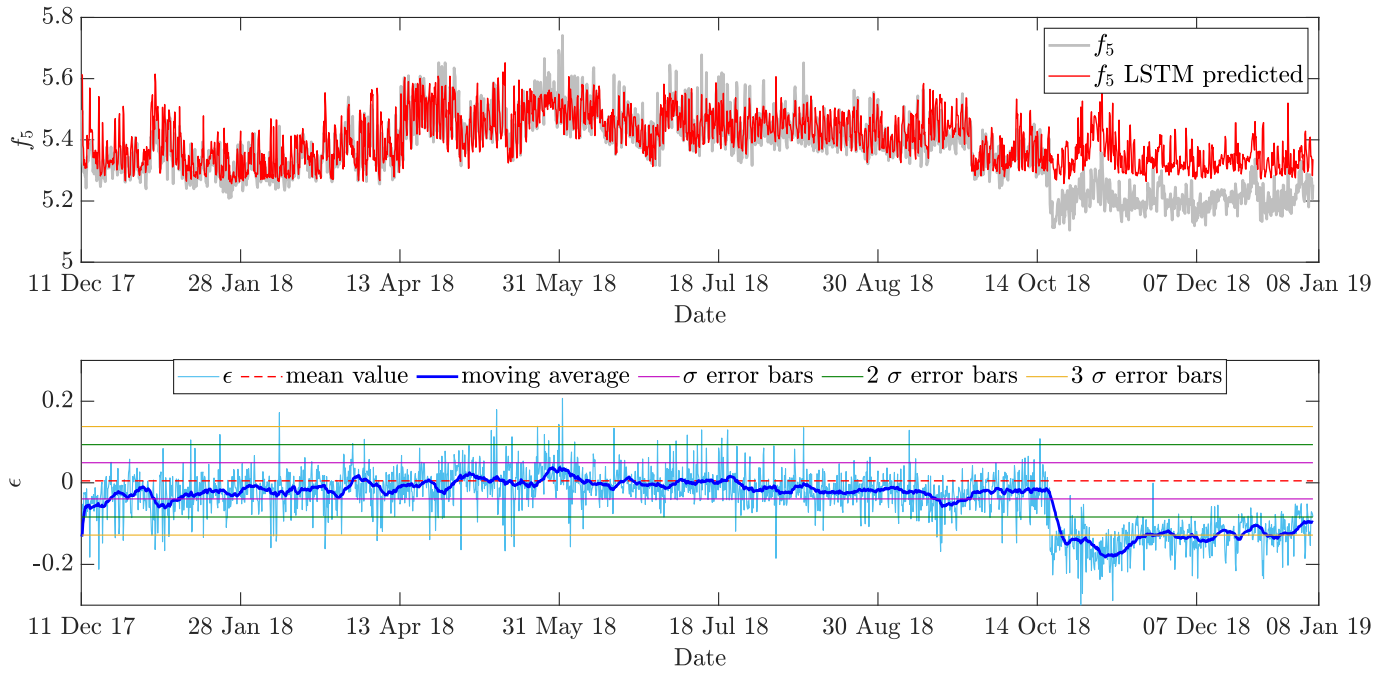

Fig. 10. LSTM model of f_5 using the collected data for f_1, f_3 and f_4 with simulated damage.

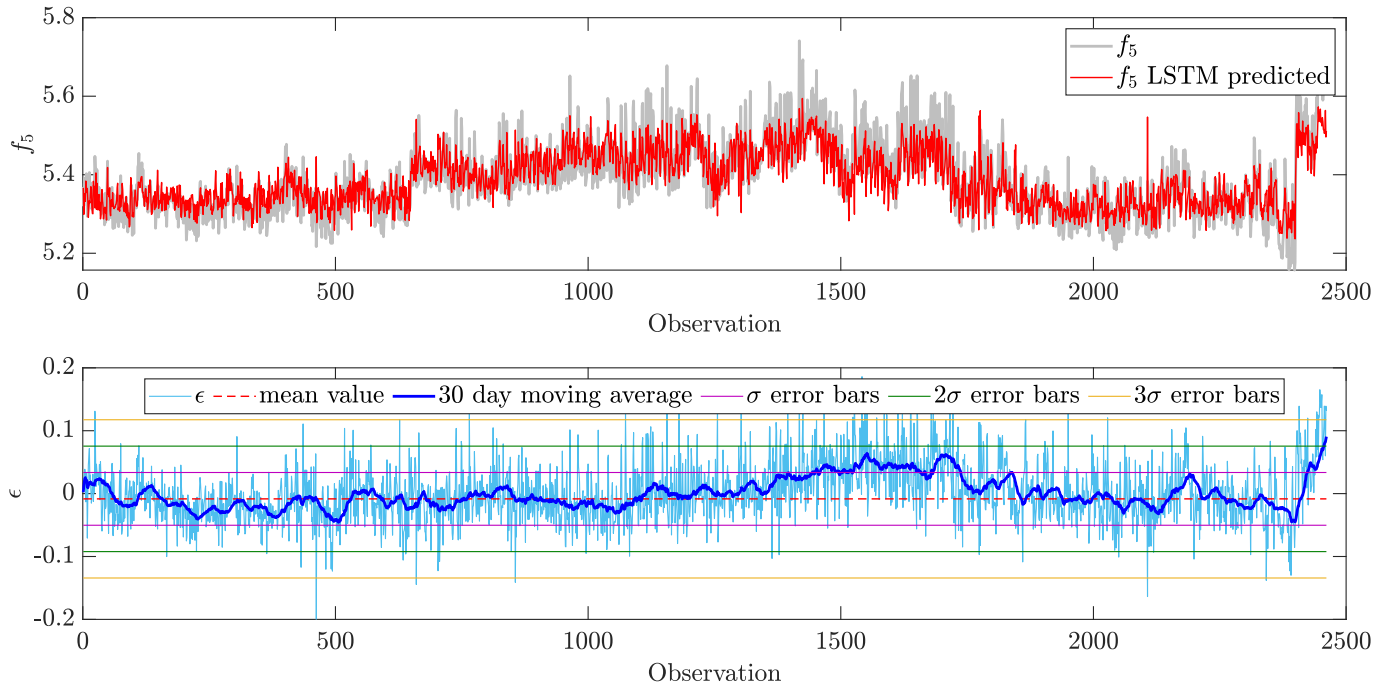

Fig. 11. LSTM model of f_5 using the collected data for f_1, f_3 and f_4 with real damage.

application on a historical reinforced-concrete masonry tower in Italy. Two regression models, the Long Short-Term Memory Neural Network and the Prophet model, are used to implement the cointegration strategy using the first five structural modes of the tower. Both models show robust regression performance regardless of the training data size and time-window period and are able to remove the temperature nonstationary dependence of the frequencies from the temperature. However, the LSTM model outperforms the Prophet model in predicting structural frequency with unseen temperature trends. Finally, the LSTM model is applied to the monitoring data of the Civic Tower of Rieti and generates stationary residuals independent of temperature fluctuations.

The investigation on the temperature dependency of Cepstral Coefficients shows that the higher-order coefficients tend to be independent of long-term temperature dependencies because of their extraction process. The discrete cosine transform acts as a filter on the spectral bins of the system, removing the long-term fluctuations due to temperature.

The study tested the damage detection approach by introducing artificial damage to a reinforced-concrete masonry tower. The cointegration method effectively detected the damage, with residual values diverging from regular mean values and exceeding set thresholds for healthy system representation. However, when considering the experimental frequency quantities collected during real damage conditions,

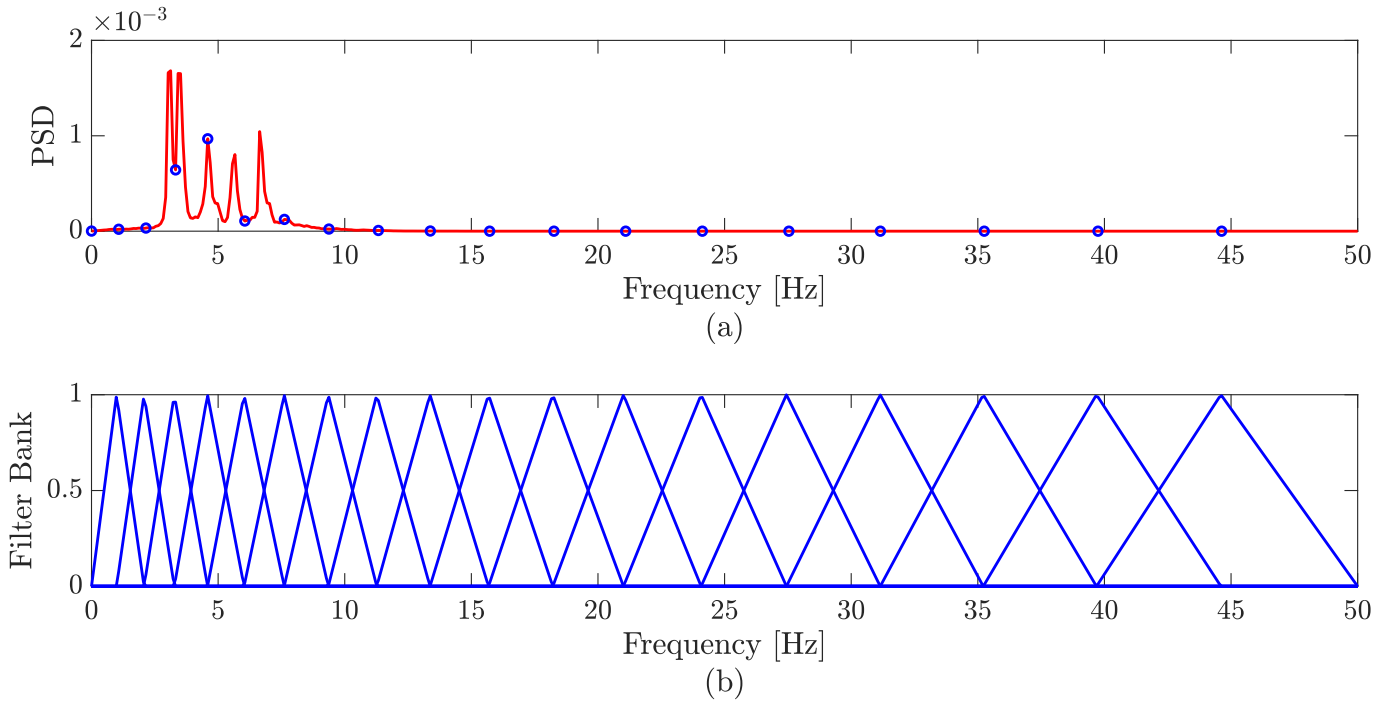

Fig. 12. Average spectrum (a) and triangular filters for the first sensor (b).

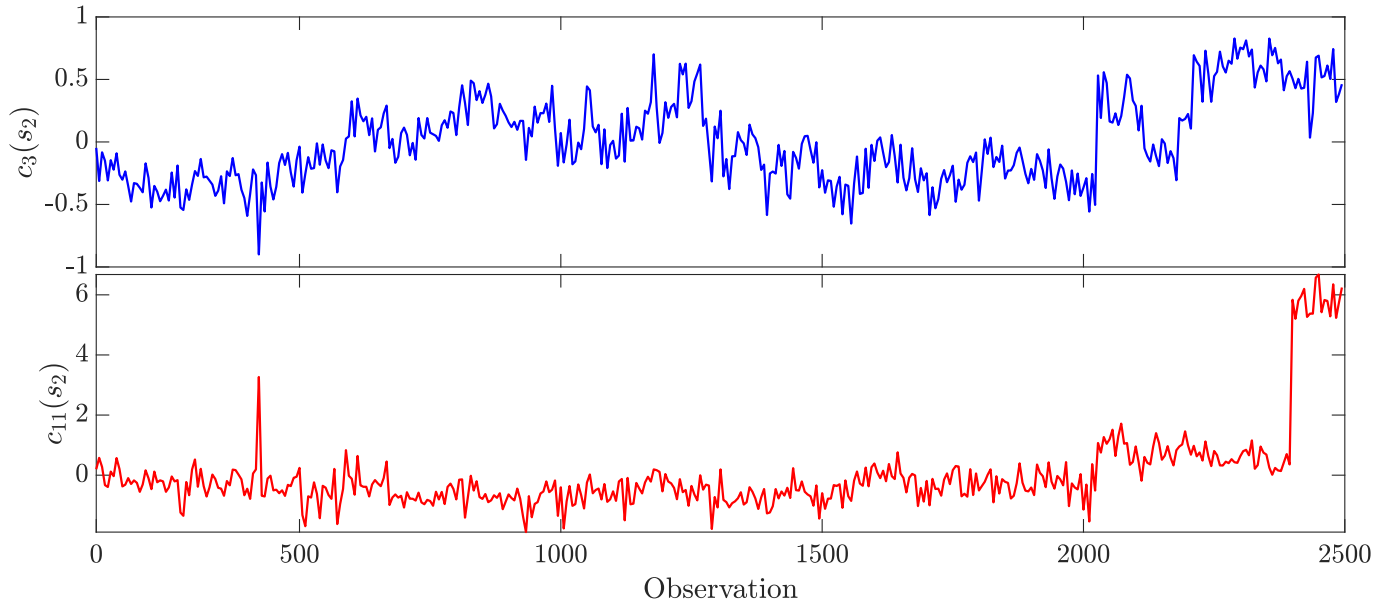

Fig. 13. Cepstral Coefficients c_3 and c_{11} time series for channel 2.

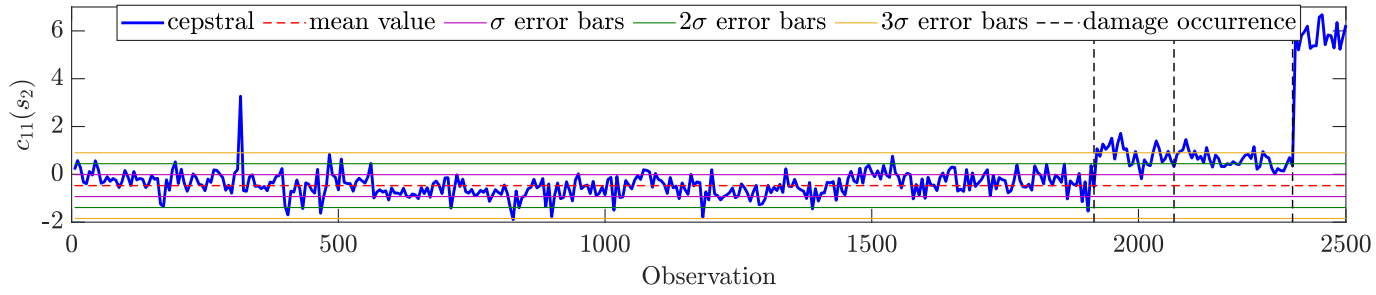

Fig. 14. Control chart for Cepstral Coefficient c_{11}.

the strategy failed to detect damage. This highlights limitations in using cointegration residuals for monitoring when damage emerges uniformly in all frequency components. In addition, higher-order Cepstral Coefficients were found to be highly sensitive features for damage detection without needing to remove temperature dependency first.

The results obtained from using Cepstral Coefficients in detecting damage in a real study case, particularly in the presence of a seismic event, are promising. Combining these features with cointegration residuals could enhance the reliability and effectiveness of damage detection strategies for civil structures. Cepstral Coefficients provide a complementary and naturally insensitive feature set to the temperature-dependent cointegration residuals. The proposed combination of these two sets of features could offer a more comprehensive and robust approach to detecting structural damage, particularly in scenarios where environmental factors or operational conditions may impact the reliability of individual features.

Declaration of competing interest

The authors declare that they have no known competing financial interests or personal relationships that could have appeared to influence the work reported in this paper.

Data availability

The authors do not have permission to share data.

References

Balsamo, L., Betti, R., Beigi, H., 2013. Structural damage detection using speaker recognition techniques. In: Proceedings of the 11th International Conference on Structural Safety and Reliability (ICOSSAR). Columbia University, New York, NY, USA.

Balsamo, L., Betti, R., Beigi, H., 2014. A structural health monitoring strategy using cepstral features. J. Sound Vib. 333, 4526–4542.

Barsocchi, P., Bartoli, G., Betti, M., Girardi, M., Mammolito, S., Pellegrini, D., Zini, G., 2021. Wireless sensor networks for continuous structural health monitoring of historic masonry towers. Int. J. Architect. Herit. 15, 22–44.

Beigi, H., 2011. Speaker Recognition. *Fundamentals of Speaker Recognition*, pp. 543–559.

Bernagozzi, G., Achilli, A., Betti, R., Diotallevi, P., Landi, L., Quqa, S., Tronci, E., 2021. On the use of multivariate autoregressive models for vibration-based damage detection and localization. Smart Struct. Syst. An Int. J. 27, 335–350.

Bogert, B., 1963. The Quefrency Alanysis of Time Series for Echoes; Cepstrum, Pseudo-autocovariance, Cross-Cepstrum and Saphe Cracking. *Time Series Analysis*, pp. 209–243.

Cabboi, A., Gentile, C., Saisi, A., 2017. From continuous vibration monitoring to FEM-based damage assessment: application on a stone-masonry tower. Construct. Build. Mater. 156, 252–265.

Civera, M., Pecorelli, M., Ceravolo, R., Surace, C., Zanotti Fragonara, L., 2021. A multi-objective genetic algorithm strategy for robust optimal sensor placement. Comput. Aided Civ. Infrastruct. Eng. 36, 1185–1202.

Coletta, G., Miraglia, G., Pecorelli, M., Ceravolo, R., Cross, E., Surace, C., Worden, K., 2019. Use of the cointegration strategies to remove environmental effects from data acquired on historical buildings. Eng. Struct. 183, 1014–1026.

Cross, E., Worden, K., Chen, Q., 2011. Cointegration: a novel approach for the removal of environmental trends in structural health monitoring data. Proc. Math. Phys. Eng. Sci. 467, 2712–2732.

Cross, E., Manson, G., Worden, K., Pierce, S., 2012. Features for damage detection with insensitivity to environmental and operational variations. Proc. Math. Phys. Eng. Sci. 468, 4098–4122.

Davis, S., Mermelstein, P., 1980. Comparison of parametric representations for monosyllabic word recognition in continuously spoken sentences. IEEE Trans. Acoust. Speech Signal Process. 28, 357–366.

Eltouny, K., Liang, X., 2023. Large-scale structural health monitoring using composite recurrent neural networks and grid environments. Comput. Aided Civ. Infrastruct. Eng. 38, 271–287.

Farrar, C., Worden, K., 2012. Structural Health Monitoring: a Machine Learning Perspective. John Wiley & Sons.

Fraile, R., Sáenz-Lechán, N., Godino-Llorente, J., Osma-Ruiz, V., Gómez-Vilda, P., 2008. Use of mel-frequency cepstral coefficients for automatic pathology detection on sustained vowel phonations: mathematical and statistical justification. In: Proc. 4th International Symposium on Image/video Communications over Fixed and Mobile Networks. Bilbao, Brazil.

Fuller, W., 2009. Introduction to Statistical Time Series. John Wiley & Sons.

García-Macías, E., Ubertini, F., 2022. Least Angle Regression for early-stage identification of earthquake-induced damage in a monumental masonry palace: palazzo dei Consoli. Eng. Struct. 259, 114119.

Gentile, C., Saisi, A., 2007. Ambient vibration testing of historic masonry towers for structural identification and damage assessment. Construct. Build. Mater. 21, 1311–1321.

Giglioni, V., Venanzi, I., Ubertini, F., 2023. Application of unsupervised learning for post-earthquake assessment of the Z24 benchmark bridge. Procedia Struct. Integr. 44, 1948–1955.

Han, Q., Ma, Q., Xu, J., Liu, M., 2021. Structural health monitoring research under varying temperature condition: a review. J. Civ. Struct. Health Monitor. 11, 149–173.

Harvey, A., Peters, S., 1990. Estimation procedures for structural time series models. J. Forecast. 9, 89–108.

Hochreiter, S., Schmidhuber, J., 1997. Long short-term memory. Neural Comput. 9, 1735–1780.

Ierimonti, L., Cavalagli, N., Venanzi, I., García-Macías, E., Ubertini, F., 2022. A Bayesian-based inspection-monitoring data fusion approach for historical buildings and its post-earthquake application to a monumental masonry palace. Bull. Earthq. Eng. 1–34.

Invernizzi, S., Lacidogna, G., Lozano-Ramírez, N., Carpinteri, A., 2019. Structural Monitoring and Assessment of an Ancient Masonry Tower, vol. 210. Engineering Fracture Mechanics, pp. 429–443.

Johansen, S., 1995. Likelihood-based Inference in Cointegrated Vector Autoregressive Models. OUP Oxford.

Kita, A., Cavalagli, N., Ubertini, F., 2019. Temperature effects on static and dynamic behavior of Consoli Palace in Gubbio, Italy. Mech. Syst. Signal Process. 120, 180–202.

Li, L., Morgantini, M., Betti, R., 2023. Structural damage assessment through a new generalized autoencoder with features in the quefrency domain. Mech. Syst. Signal Process. 184, 109713.

Oppenheim, A., Buck, J., Schafer, R., 2001. Discrete-time Signal Processing, vol. 2. Prentice Hall, Upper Saddle River, NJ.

Pallarés, F., Betti, M., Bartoli, G., Pallarés, L., 2021. Structural health monitoring (SHM) and Nondestructive testing (NDT) of slender masonry structures: a practical review. Construct. Build. Mater. 297, 123768.

Pan, Q., Bao, Y., Li, H., 2023. Transfer learning-based data anomaly detection for structural health monitoring. Struct. Health Monit., 14759217221142174

Quqa, S., Landi, L., Diotallevi, P., 2021. Automatic identification of dense damage-sensitive features in civil infrastructure using sparse sensor networks. Autom. ConStruct. 128, 103740.

Shi, H., Worden, K., Cross, E., 2016. A nonlinear cointegration approach with applications to structural health monitoring. J. Phys. Conf. 744, 012025.

Silva, M., Santos, A., Santos, R., Figueiredo, E., Costa, J., 2021. Damage-sensitive feature extraction with stacked autoencoders for unsupervised damage detection. Struct. Control Health Monit. 28, e2714.

Taylor, S., Letham, B., 2018. Forecasting at scale. Am. Statistician 72, 37–45.

Tronci, E., De Angelis, M., Betti, R., Altomare, V., 2020a. Vibration-based structural health monitoring of a RC-masonry tower equipped with non-conventional TMD. Eng. Struct. 224, 111212.

Tronci, E., De Angelis, M., Betti, R., Altomare, V., 2020b. Semi-automated operational modal analysis methodology to optimize modal parameter estimation. J. Optim. Theor. Appl. 187, 842–854.

Tronci, E., Beigi, H., Feng, M., Betti, R., 2022. A transfer learning SHM strategy for bridges enriched by the use of speaker recognition x-vectors. J. Civ. Struct. Health Monitor. 1–14.

Turrisi, S., Cigada, A., Zappa, E., 2022. A cointegration-based approach for automatic anomalies detection in large-scale structures. Mech. Syst. Signal Process. 166, 108483.

Ubertini, F., Comanducci, G., Cavalagli, N., Pisello, A., Materazzi, A., Cotana, F., 2017. Environmental effects on natural frequencies of the San Pietro bell tower in Perugia, Italy, and their removal for structural performance assessment. Mech. Syst. Signal Process. 82, 307–322.

Vishwas, B., Patel, A., Vishwas, B., Patel, A., 2020. Prophet. *Hands-On Time Series Analysis with Python: from Basics to Bleeding Edge Techniques*, pp. 375–394.

Zhang, G., Harichandran, R., Ramuhalli, P., 2011. Application of noise cancelling and damage detection algorithms in NDE of concrete bridge decks using impact signals. J. Nondestr. Eval. 30, 259–272.